Journal of Mechanical Engineering and Sciences (JMES)
e-ISSN: 2231-8380; Volume 2, pp. 237-250, June 2012

MONITORING AND ASSESSMENT OF ACOUSTIC EMISSION SIGNATURES DURING FATIGUE MECHANISM OF API5LX70 GAS PIPELINE STEEL

M.F.M. Yusof[1,2], N. Jamaludin[1], S. Abdullah[1], Z.H. Hanafi[1], M.S.M. Zain[1]

[1]Department of Mechanical and Materials Engineering
Faculty of Engineering and Built Environment, Universiti Kebangsaan Malaysia,
43600 UKM, Bangi, Selangor, Malaysia.
[2]Faculty of Mechanical Engineering, Universiti Malaysia Pahang,
26600 UMP, Pekan, Pahang, Malaysia;
Phone: +6019-7750510, Fax: +609-4242202
E-mail: fadhlanyusof@gmail.com

ABSTRACT

The detection of an early fatigue phenomenain a gas pipeline is crucial to avoid catastrophic consequences. Therefore,appropriate inspection is needed to assess the fatigue phenomena in a gas pipeline system. The acoustic emission (AE) technology is expected to be suitable in this regards. This paper presents the monitoring and assessment of AE signatures during fatigue mechanism of gas pipeline material, API 5L X70 steel. The stress amplitude of 65, 60, 58 and 53% of ultimate tensile strength were done in order to observe the AE activity during the fatigue mechanism. The field measurements were also being done by commencing the AE signatures from the in-operation gas pipeline for comparison purpose. Based on the correlations of AE signatures and fatigue mechanism, it was found that the AE activities generated during fatigue mechanism were divided into three different stages. Analysis of the AE features and statistical parameters have shown that the kurtosis values of the time domain AE signatures from the third stage of the fatigue mechanism were different from the field measurement. This results show that application of the kurtosis was expected to be able to detect the time domain AE signatures from crack stage.

***Keywords*:** Acoustic emission, fatigue, API5L X70 steel, statistical parameter.

INTRODUCTION

Fatigue is a common failure mechanism in engineering structures including gas pipelines. Even the statistical history did not prove that fatigue failure is a major problem in gas pipelines; it cannot be ignored because it can happen rapidly without any indication and caused a catastrophic failure (Muhlbauer, 2004). Conventionally, inspection technique of in-operation gas pipeline gives only information about noticeable crack. However, it is not essential to detect the noticeable cracks because gas pipelines already considered failure. Thus, an early detection of fatigue crack is crucial and monitoring technique. The crack initiation mechanism can be influenced by inclusion and pores in some materials (Chan, 2009). Both size and spacing of inclusions and pores affects localized straining and crack incubation life. Generally, bigger size and smaller spacing of inclusions and pores increase the number of plastic local straining and shorten the crack incubation life. In materials with less (approximately zero) numbers of inclusion and pores, crack tends to initiate from the persistent slip

band (PSB). The extension of intrusion and extrusion have caused slip plane cracking to extend to a few grain diameters and then change to the continuum mechanism of crack propagation (Janssen et al., 2004). During crack growth, micro mechanism involved and captured an attention for studies is microplastic at the crack tip and crack closure phenomena.

Acoustic emission (AE) technique is suitable because of the detect micro phenomena in materials. AE was defined as the radiation of elastic waves produced by a localize source in materials due to dynamic local arrangement of its internal structure (Baranov et al., 2007). Source of AE can be classified into a microscale and macroscale. Microscopic source refers to the micro-mechanism such as dislocation motion, slip formation, micro crack initiation and,etc. (Kalyanasundaram et al., 2007). Huang et al. (1998) had summarized that AE activities generated during fatigue of materials caused by various mechanisms, which can be divided into three stages. The first-stage show high AE activity due to the dislocation movement and cyclic softening and hardening. This phenomena happens at the first few cycle before the cyclic curve gets stabilized. The second stage corresponds to the crack incubation stage where steady-state dislocation happens and results in formation of micro voidand micro crack.This phenomena leads to nearly quiet AE activity and only small AE activities appear. Ai et al. (2010) found that a few burst type AE signals appear at this stage due to the micro crack formation. During the last stage, crack start to grow and propagate, and AE activities were actived. Many AE generated at this stage is a result from micro crack coalescence, fracture along grain boundary, crack tip plastic deformation and also crack closure. The crack initiation phenomena can be detected by rapidly increased of AE activity at positive peak stress during cyclic loading to Incoloy 901 (Berkovits and Fang, 1995). It was followed by AE activity with clear boundary around zero stresses, which correspond to crack closure phenomena. After crack was propagate, an increasing in crack length might affect the crack closure phenomena. Therefore, study on the effect of crack length to the crack closure phenomena in alluminium alloy LY12CZ had been done by Chang et al. (2009) using AE monitoring. Recognitions of AE behavior during crack closure were taken as a good guideline by Roberts and Talebzadeh (2003) in order to study the growth of crack.

AE and fatigue crack mechanism by extracting AE features from generated AE signatures. AE features such as hits (number of AE activities), count, and count rates have been successfully correlated with crack closure phenomena, micro-phenomena during fatigue mechanism, crack growth and life prediction. However, there was lacked of finding of the analysis of the statistical parameters of the time-domain AE signatures generated during fatigue crack mechanism. In case of fatigue and vibration analysis, statistical parameters are frequently used to characterize and classify random signal (Nuawi et al., 2009). Elangovan et al. (2011) summarized that kurtosis of time domain vibration signal is a good measurement for tool condition monitoring. This paper presents the monitoring and assessment of AE time domain signatures during fatigue mechanism of a gas pipeline material, API 5L X70 steel in laboratory test and normal operation field measurement. Therefore, the correlation between AE signatures and fatigue mechanism were done. The behavior of the time domain AE signatures from different stages of the fatigue mechanisms in laboratory tests will be investigated in-operation gas pipelines.

METHODOLOGY

Experimental Setup

The fatigue test specimens were prepared by cutting the test coupon of API 5L X70 steel in longitudinal direction. It was milled into a plate and wire cut to dimension according to ASTM E466-07 standard. Figure 1 shows the data acquisition setpu in the laboratory. The wide band piezoelectric sensor was mounted on the surface of fatigue specimen using vacuum grease and calibrated by pencil lead break testing (ASTM E976-05). Threshold level of 44.1 dB was set after background noise level was detected. Recorded AE signals were amplified by preamplifier with 34 dB gain and it was analyzed by AMSY-5 from VallenSysteme. AE signals captured were filtered within frequency range from 25 to 850 kHz with a sampling rate of 5 MHz. The fully reverse fatigue test (R = -1) with frequency of 5 Hz and stress amplitude of 65, 60, 58, and 53% from its ultimate tensile strength were done based on ATSM E466-07. The cyclic stress amplitudes were varied in order to observe on the pattern of AE activities. The stress ratio, R of -1 was selected in order to observe the behavior of AE spectrums generated from both tension and compression mode.

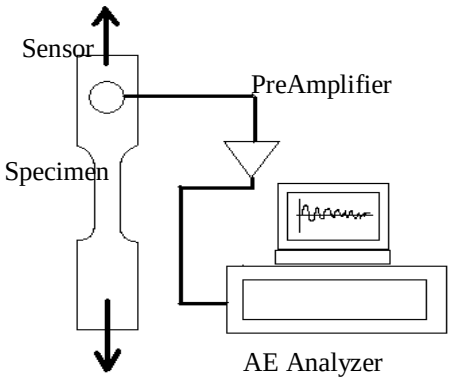

Figure 1. Data Acquisition setup in the laboratory.

Field Measurement Setup

It was obvious to capture AE signatures at the junction of a gas pipeline according to API 570 in the field. Measurement was done by mounting the wide band piezoelectric sensor on the surface of pipeline using vacuum grease. The sensor mounting was calibrated by pencil lead break testing according to ASTM E976-05 standard. All controlled parameters in the AE acquisition setup similar to the laboratory test. However, in field measurement, lower background noise was detected. So, threshold setting was decreased to 40dB. Figure 2 shows the field measurement setup.

Figure 2. Field measurement setup.

Feature Extraction

In this study, the correlation between the AE activities and fatigue mechanism were plotted in the 3D histogram. Then, AE signatures were grouped based on those stages for feature analysis purpose. The time domain AE signatures from laboratory fatigue test were divided into seven groups based on different stages of crack mechanism. Then the grouped time domain AE signatures from fatigue mechanismwere combined with the time domain AE signatures from the in-operation gas pipeline for feature extraction analysis. Figure 3 shows how AE features were extracted from the time-domain signatures. AE energy is the area under the graph within the duration of time domain AE signatures. Among all those AE features, only two features were selected for analysis. The selected AE features werethe AE maximum amplitude and AE energy.

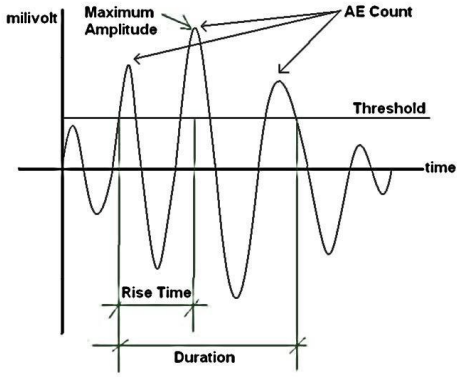

Figure 3. Time domain and frequency domain AE signatures.

AE maximum amplitude was chosen for study because AE maximum amplitude can be related to the intensity of source. It was expected that AE maximum amplitude given a different value for a different fatigue mechanism. Energy of AE signal gives an advantage compare to another feature because it can directly be related with physical parameter of AE sources. In this study, AE energy will be presented in electrical unit (eu). Therefore, the area under the graph of AE time domain signatures in Eq. (1) will be converted into unit eu by using Eq. (2). It was explained that the threshold levels of field measurement were different from laboratory fatigue test. Thus, the AE energy value from field measurement signals will be calculated based on the laboratory threshold to avoid the error from the analyzed data.

$$E = \frac{1}{R}\int_0^\infty V(t)^2 . dt \quad (1)$$

$$1\ eu = 10^{-14}V^2 \quad (2)$$

The most commonly used statistical parameters are mean, standard deviation, root mean square (rms), skewness, kurtosis, and crest factor (Nuawi et al., 2009). However, the standard deviation, kurtosis and skewness were selected for this study. The definition and formula of those statistical parameters are as follows.

(a) Standard deviation – This is defined as measurement of data spreading about mean value. This is also defined as a measure of the power content of the

vibration signal (Elangovan et al., 2011). The standard deviation is expressed as Eq. (3).

$$\text{Standard Deviation} = \left(\frac{1}{n-1}\sum_{j=1}^{n}(x_j - \bar{x})^2\right)^{\frac{1}{2}} \quad (3)$$

(b) Kurtosis – Kurtosis is a measure the spikeness of the data. It is used for detection of the fault symptoms because of highly sensitive to the high-amplitude event. Thus, kurtosis was sensitive in detecting faulty phenomena, which referred as micro phenomena during fatigue mechanism.

$$\text{Kurtosis} = \frac{1}{n(\text{Standard Deviation})^4}\sum_{j=1}^{n}(x_j - \bar{x})^4 \quad (4)$$

(c) Skewness –It is the measure of symmetry or the data distribution as expressed in Eq. (5).

$$Skewness = \frac{1}{n(StandardDeviation)^3}\sum_{j=1}^{n}(x_j - \bar{x})^3 \quad (5)$$

The value of *n* in Eq. (3)-(5) corresponds to the number of samples in single signatures. The time domain AE signatures were cut to avoid the effect of unwanted signatures in analysis. Thus, the number of samples, *n* in each signal in this study was 2500.

RESULTS AND DISCUSSION

AE Signatures and Fatigue Mechanism

Correlation between AE activities and fatigue mechanism is presented in this section. Figure 4 shows the AE activities during the fatigue test with stress amplitude of 65% of ultimate strength. It is clearly seen that the numbers of captured AE signatures were high during the first few cycle. It is found that this phenomena happens until 25th cycles. Starting from 25th cycle until 200 cycles, the AE activities are not as active as previous. Only small numbers of AE activities were captured within this range. AE activities become active again starting from 200th cycles, and the number of AE activities found increased rapidly starting from 1920th cycles. However, most of the activities after 1920th cycle captured at positive peak stress amplitude. Similar trend is shown by AE activities during the fatigue test with stress amplitude of 60% ofultimate strength in Figure 5. It is found that AE activities active at the first few cycles. This phenomena can be observed starting from the first cycles until 20th cycles. After 20th cycles, AE activities were not active, and only small number of AE activities were captured. This phenomena was happened until 100th cycle and AE activities start becoming active again after that. After 3500th cycles, AE activities become more active. There wasthe high number of AE activities per cycle can be found after 3500th cycles. At the last stage before experiment was finished, high numbers of AE activities were also found at the positive peak stress amplitude.

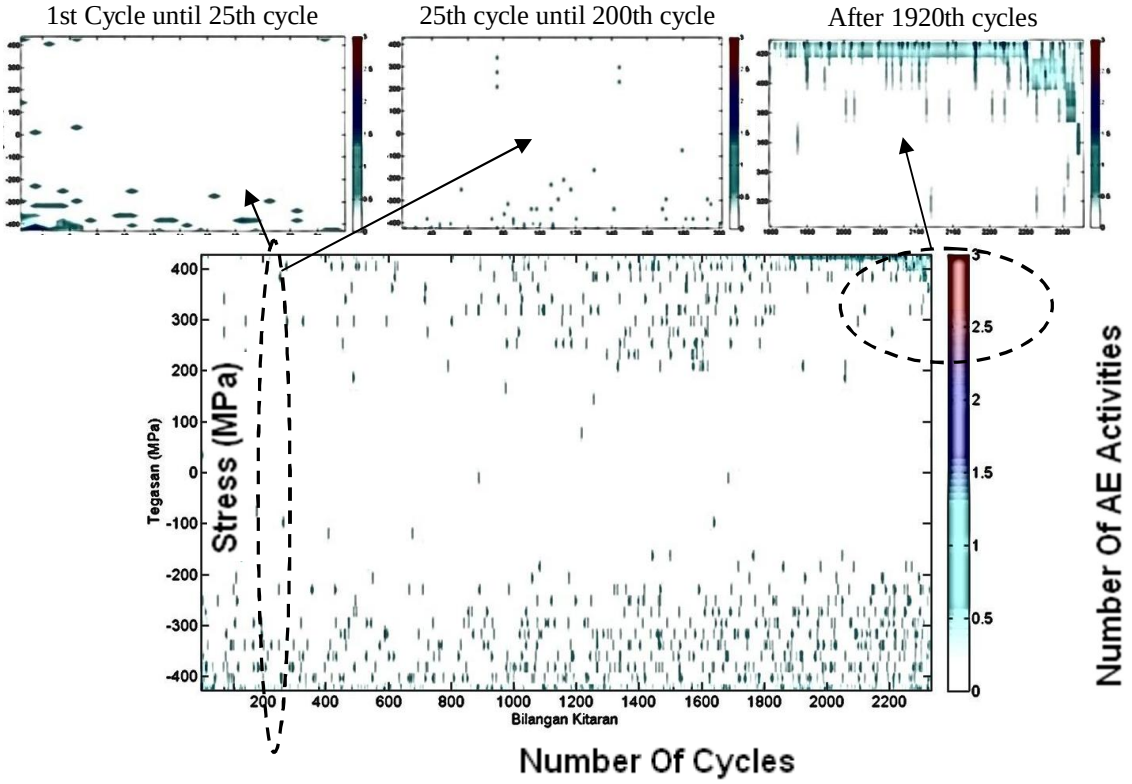

Figure 4. Acoustic emission activities during API 5L X70 fatigue test 1 with stress amplitud of 437.5MPa.

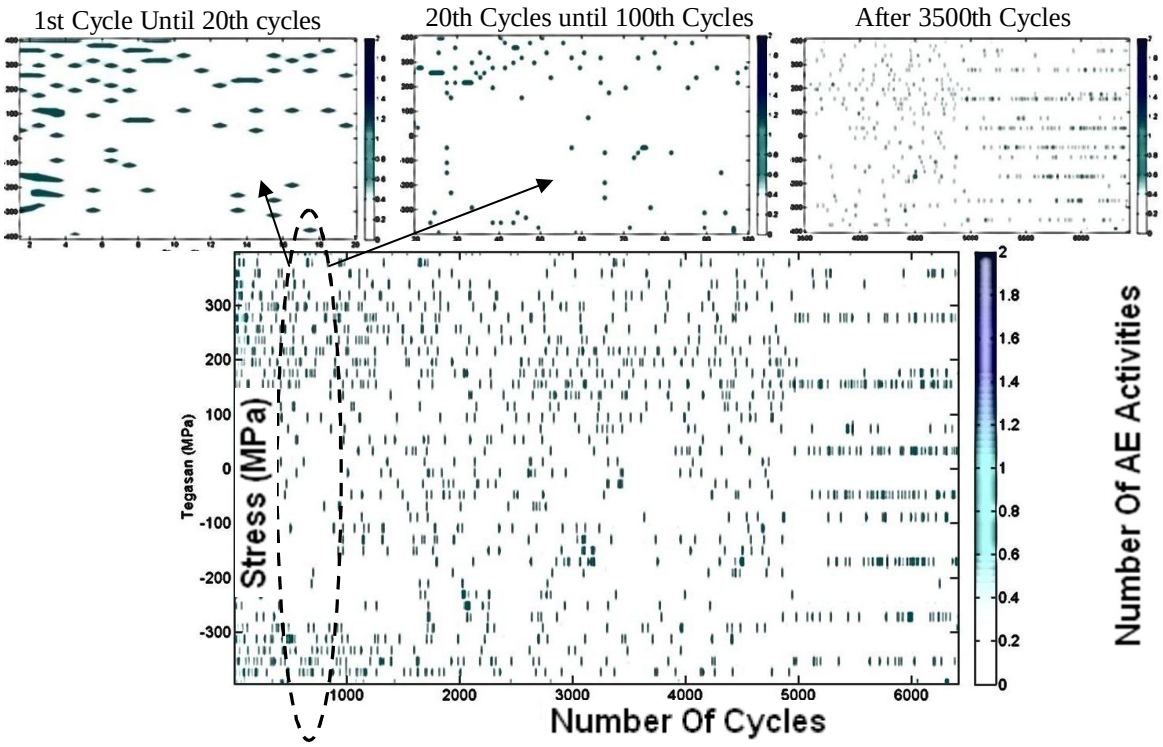

Figure 5. Acoustic emission activities during API 5L X70 fatigue test 2 with stress amplitud of 406.25MPa.

The AE activities has shown an active behavior starting from the first cycle until 8th cycles in Figure 6. Starting from 8th cycle until 1000th cycles, AE activities become inactive only small numbers of AE activities per cycle were found within this cycle range. Begin from 29379th cycles, the different phenomena from previous tests were found. At this stage, all captured AE activities were clearly divided into three divisions. The first division shows a high number of AE activities within stress amplitude between 390 MPa until 391 MPa. The second division, active AE activities around 114.2 MPa until 115.5 MPa while the third division stress amplitude of -318 MPa until -315.5 MPa. AE activities from fatigue test with stress amplitude of 53% from ultimate strengtis shown in Figure 7. It is found that AE activities were active starting from the first cycle until 20th cycles. AE activities become inactive until the 47088th cycle only small numbers of AE activities were captured at this stage. Starting from 47088th cycle until 66057th cycle, AE activities start to be active again. The number of captured AE activities per cycle was increased in every cycle during this stage. At the final stege, similar phenomena as presented in Figure 6.

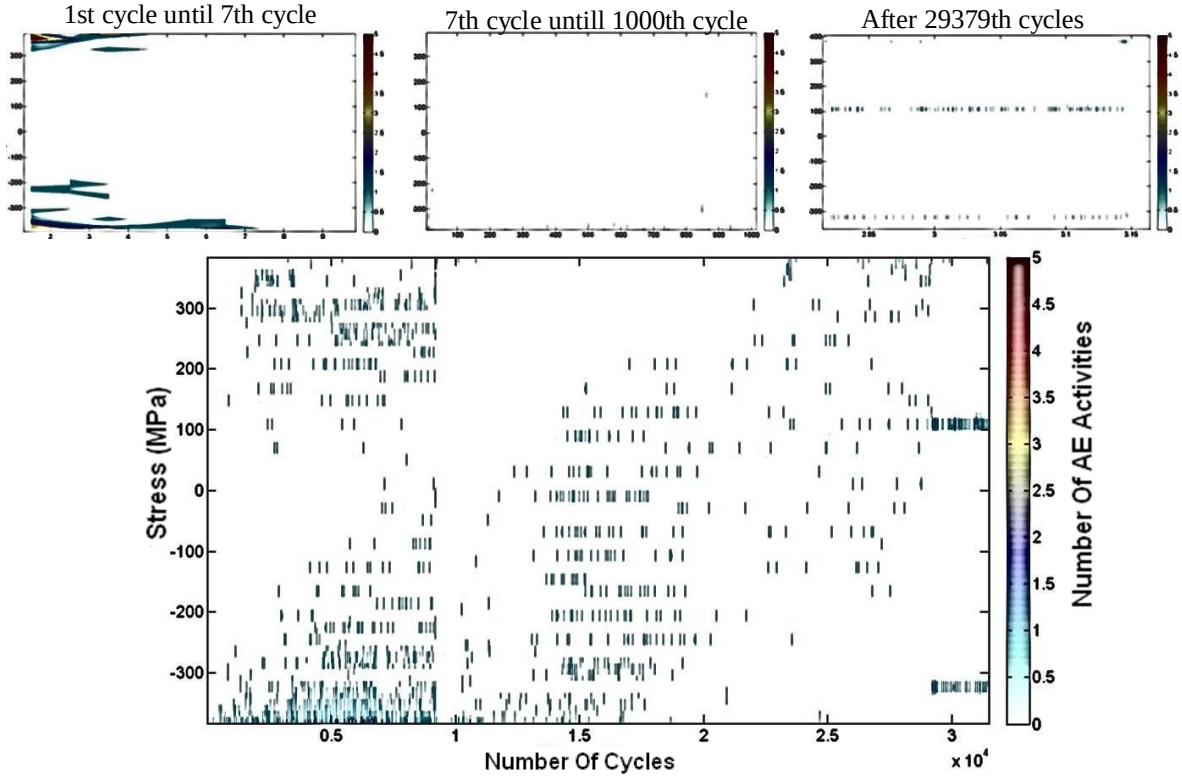

Figure 6. Acoustic emission activities during API 5L X70 fatigue test 3 with stress amplitude of 390.6 MPa.

Prior to crack initiation, all tests show high AE activities in both tension and compression mode. In Figure 8, it is found that the cyclic softening phenomena washappened at this stage. This is happened because of the values of cyclic peak strain amplitude started to increase in every cycle during this stage. Therefore, AE generated due to the slip plane and microplastic formation before the crack nucleated. AE activity at compressive peak stress is due to Bauschinger effect, which is the phenomena where AE generated due to change of strain direction (Berkovits and Fang, 1995). It is presented that at the final stage, there is clear separation of AE activities detected at

stress around zero during fatigue test 3 and 4. The detection of AE activities around zero stresses is happening due to crack closure phenomena where upper crack surface contacted with lower crack surface during unloading. Phenomena of crack opening or closure also found by Chang et al. (2009) and Berkovits and Fang (1995) where it was detected at stress or loading around zero.

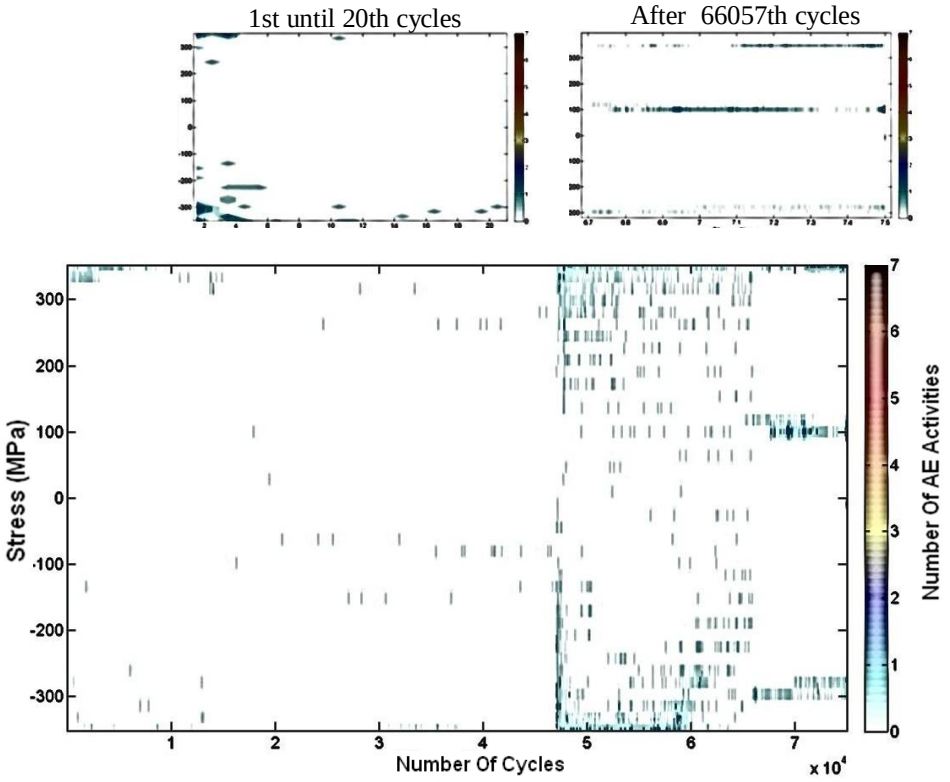

Figure 7. Acoustic emission activities during API 5L X70 fatigue test 4 with stress amplitud of 359.4MPa.

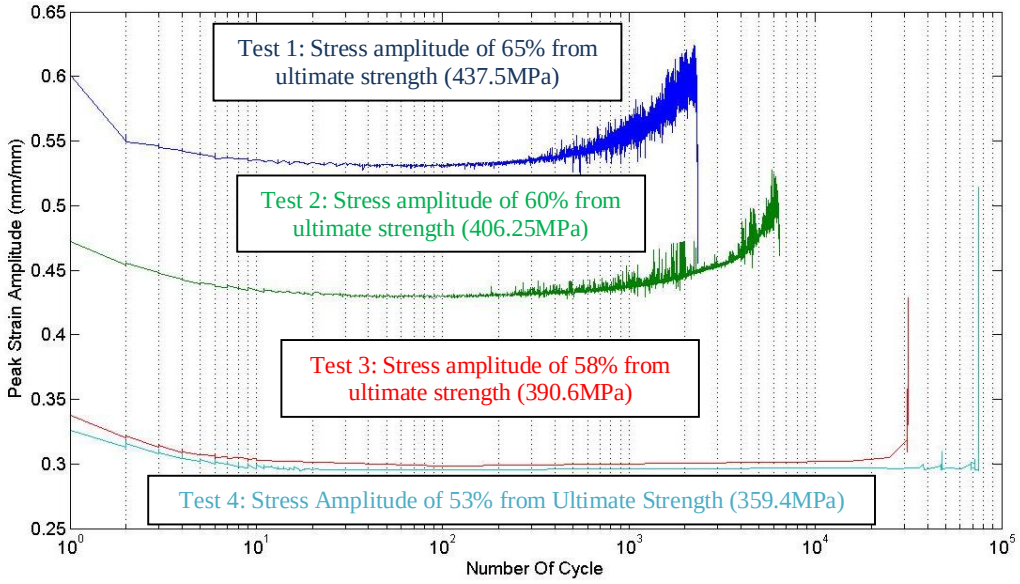

Figure 8. Cyclic peak strain amplitudes respond during fatigue test.

The fatigue mechanism can be divided into three different stages. At the first stage, cyclic softening washappened during the first cycle and followed by cyclic hardening phenomena for several cycles. AE activities re active but the numbers of captured AE activities per cycle were decreased during cyclic hardening. At the second stage, the peak strain amplitude is shown the nearly flat respond. There is no obvious change in strain during this time. This stage was called crack incubation stage where only small number of AE were captured because of pile-up breakage and formation of micro void (Kalyanasundaram et al., 2007). However, the cyclic softening phenomena start to exist at the end of the second stage where high numbers of AE activities captured during this time. The most of the captured AE signatures from slip plane formation because of there is an obvious change in strain amplitude, which indicates the small plastic deformation phenomena. During the last stage (the crack formation and propagation stage), AE signatures captured from crack initiation and propagation, crack closure, and compressed crack phenomena. It is found that the higher value of stress amplitude given the higher value of peak strain amplitude response and longer duration of crack incubation stage. This phenomena shows a good agreement with Chan (2009) where the crack incubation stage decreases with increase of the local straining. The increase in cyclic stress amplitude increase the amount of local staining.

Time Domain AE Signatures Behavior

The AE activities from all fatigue tests were divided into three different stages. At the first stage in the first few cycle, there were high AE activities due to cyclic softening at the first few cycle. This phenomena caused by the start-and-stop effect, which affect to the low cycle fatigue failure (Zhong et al., 2005). Although, the start-and-stop effect considered insignificant because of this effect is not happened in the normal operating gas pipeline. Therefore, it is decided to neglect the time domain AE signatures. The time domain AE signatures from stage of crack incubation, microplastic and slip plane formation, and crack propagation and in-operation gas pipeline were selected for analysis. AE signatures from fatigue test 4 with stress amplitude of 53% from ultimate strength is selected for analysis due to the most obvious boundary that separates the different stages in fatigue mechanism in this case. The time domain AE signatures from different stages and different mode (tension or compression) is shown in Figure 9. One group for the time domain AE signatures from the in-operation gas pipeline is labeled as AEFM. Twenty AE signatures with similar appearance were selected from each group for analysis. The behavior of time domain AE signatures generated from fatigue test 4 is shown in Figure 10. It was clear that AE signatures generated from different stages in fatigue mechanism are the burst type AE signals. Figure 10(a) and (b) show time domain AE signatures of AE2T and AE2C group respectively. Both groups are corresponded to the second stage of the fatigue mechanisms in tension mode and compressive mode. It is observed that time domain AE signatures from AE2T group have short decay time compared to AE2C group signatures. The time domainAE signatures from both groups show the lowest amplitudes among time domain AE signatures from other groups. In another observation, AEPT group signatures in Figure 10(c) show a longest duration among all other group time domains AE signatures with longest rise and decay time. The shapes of the signals are quite similar with AE2T group time domain signatures but they have a different in amplitude's values. In the Figure 10(d), AEPB group time domain, signatures show the similar shape with AE2C

group time domain signatures. Although, comparison between AEPT and AE2T group time domain signatures, AEPB group time domain signatures have higher amplitudes, compare to AE2C group time domain signatures.

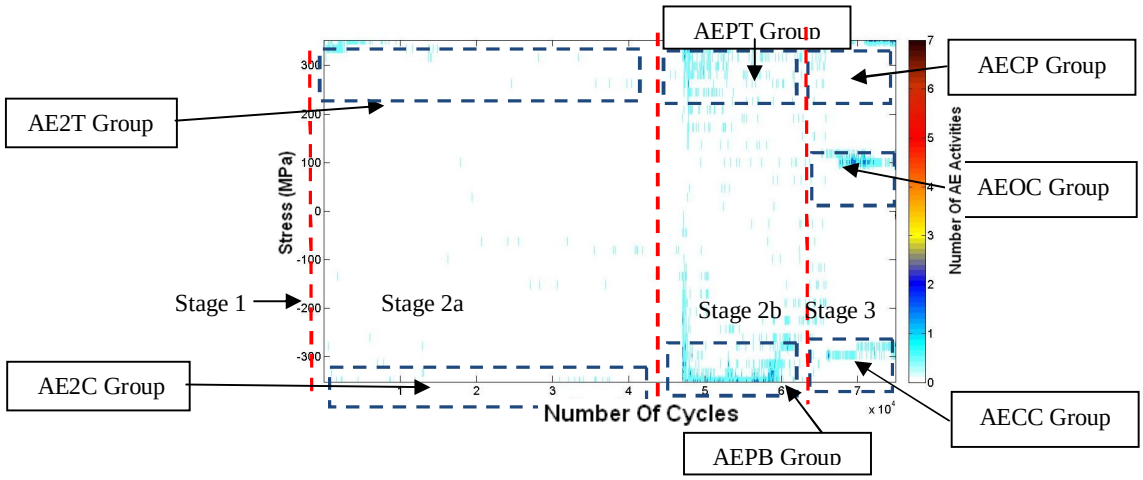

Figure 9. Group separation of microphenomena during fatigue mechanism of API 5LX70 (Specimen 4).

The time domain AE signatures from AE2T and AE2C groups correspond to the time-domain signatures from crack incubation stage show the lowest amplitudes compared to other group's time domain AE signatures. The time domain AE signatures from AE2T group shows the shortest duration. It has been stated that during crack incubation stage, there is a steady-state dislocation cause AE activity nearly quiet (Kalyanasundaram et al., 2007). Only AE signatures from pile dislocation breakage and micro void formation are appeared. Janssen et al. (2004) revealed that the formation of micro void initiates from the phenomena of microplastic in single grain followed by the pile up dislocation phenomena in a stress concentration at the grain boundary. At this point, any increasing in stress break the pile up and then micro void occurs between the grains.

Baranov et al. (2007) found that annihilation of dislocation with size of 10^{-8} to 10^{-5}m long produces time domain AE signatures with small amplitudes and duration of 5 x 10^{-5}µs. The word annihilation of dislocation refers to the dislocation breakage. Therefore, AE signatures from AE2T group, the source of time domain AE signatures are the pile up dislocation breakage. It is found that there was very small plastic deformation occur prior to crack formation. The time domain AE signatures from AE2T and AEPT group show the different in amplitudes and duration due to the Bauschinger effect occur at compressive peak stress (Berkovits and Fang, 1995). The similar shape of time domain AE signatures from AE2C and AEPB groups are due to Bauschinger effect. The time domain AE signatures from AECP, AEOC and AECC group were shown in Figure 10(e-g) respectively. In crack stage, all time-domain signatures show a short burst behavior with very short rise time. In Figure 10(e), the time domain AE signatures from AECP group produces very high amplitudes signals followed by AEOC group in Figure 10(f) with similar shape. In Figure 10(g), time domain AE signatures from AECC show the lowest amplitudes with nearly similar shape with AE2C group. During crack initiation, AE burst type with very high amplitude and energy appeared(Ai

et al., 2010; Maslov and Gradov, 1986) while for crack closure phenomena, AE burst from crack closure phenomena have less amplitudes values (Lee et al., 1995; Chang et al., 2007). AE signatures from AECP and AEOC groups have a similar burst behavior and shape but different in amplitude values. Figure 10(h) shows time domain AE signatures captured from the normal operating condition of gas pipeline during field measurement. It shows the very high-amplitude burst type signal compared to AE signatures from AECP group. AE signatures from the normal operating condition of gas pipeline show a smooth pattern with less complexity.

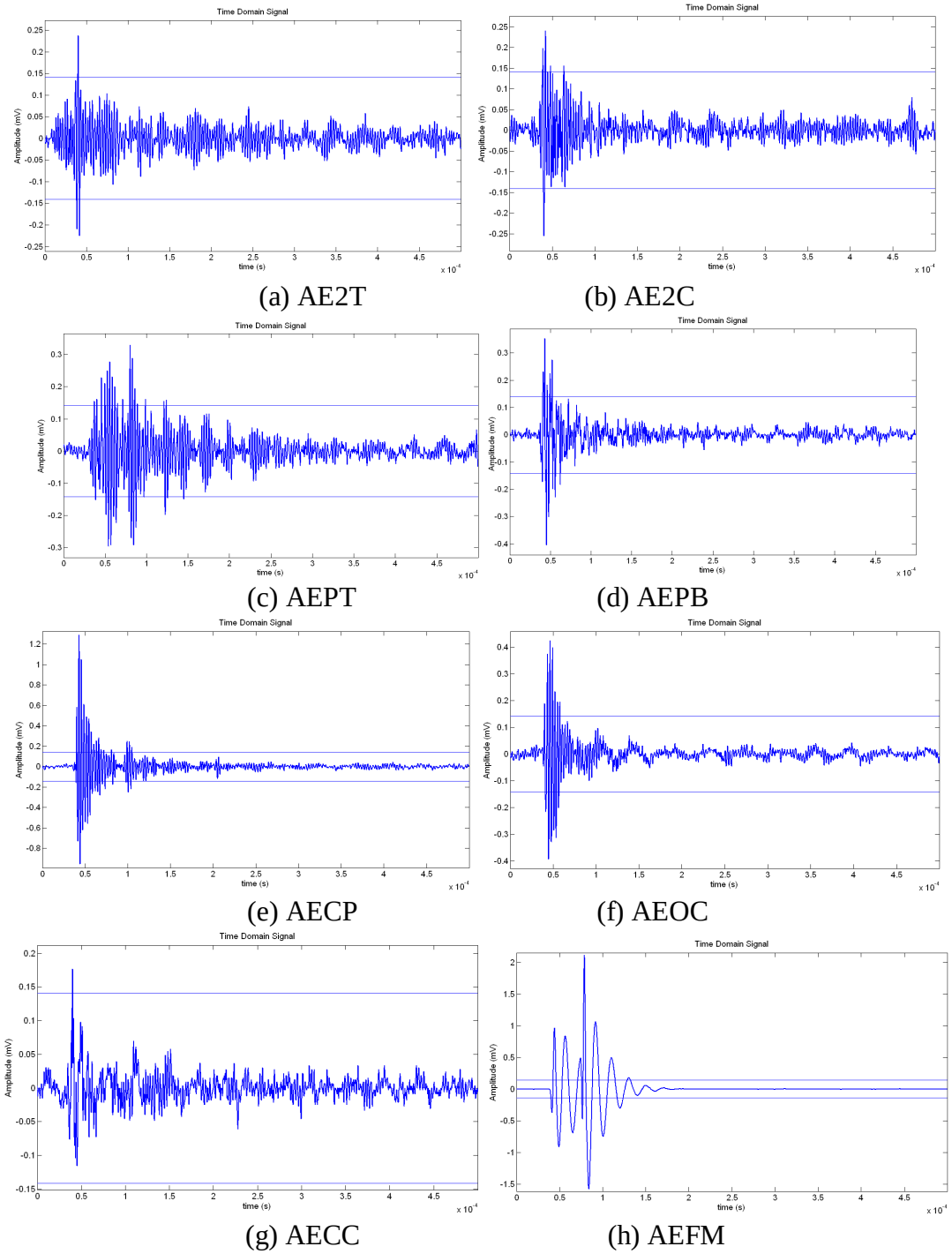

(a) AE2T (b) AE2C

(c) AEPT (d) AEPB

(e) AECP (f) AEOC

(g) AECC (h) AEFM

Figure 10. Acoustic emission signatures during test 1 fatigue and field measurement.

Feature Extraction

AE maximum amplitude and energy extracted from time domain signatures, which is presented in Table 1. Mean value of AE maximum amplitude from AE2T group is 47.9 dB while the value is 46.08 dB for AE2C group. During the stage of microplastic and slip plane, mean value of AE maximum amplitude is increased. The initiation and propagation of crack from AECP group given mean value of AE maximum amplitude os 63.37dB. The maximum amplitude value for AEFM group shows the highest mean value of 64.84 dB. Mean of AE energy both fatigue mechanism and in-operation gas pipeline show the similar pattern with mean of maximum amplitude. In crack incubation stage, mean of AE energy from AE2T group is 31.52 eu while the value drop to 30.82 eu for AE2C group. At the stage of microplastic and slip plane formation, the mean of AE energy from AEPT and AEPB groups increased. The interesting finding was found where the mean of AE energy from the normal operating gas pipeline is far higher than crack propagation stage with value of 2522 eu.

Table 1. Range and mean value of AE maximum amplitude and energy.

Signal Group	Maximum Amplitude (dB)	Mean of Maximum Amplitude (dB)	Energy (eu)	Mean of Energy (eu)
AE2T	47.1 - 48.6	47.91	20.9 - 45.3	31.52
AE2C	44.1 - 48.3	46.08	17.0 - 45.2	30.82
AEPT	50.1 - 50.9	50.38	125 - 182	156.7
AEPB	50.1 - 62.6	53.74	46.4 - 278	178.56
AECP	61.4 - 64.8	63.37	481 - 1210	778.2
AEOC	52.4 - 57.7	54.29	75 - 293	117.72
AECC	44.5 - 48.3	46.02	9.59 - 39	20.53
AEFM	60.3 - 68.2	64.84	1070 - 3820	2522

Mean of AE maximum amplitude and energy from the in-operation gas pipeline was higher than the values from the fatigue mechanism. When neglect the last stage of fatigue mechanism, AE maximum amplitude and energy show an obvious different from the in-operation gas pipeline. However, detection of a faulty symptoms are the lower value than normal operating condition, which is not essential. This is because of the lower maximum amplitude and energy values always being misunderstood as a noise. This shows that AE maximum amplitude and energy are sensitive in differentiate three different stages from crack mechanism but unsuitable to differentiate between the normal and fatigue conditions of gas pipeline.

The range and mean value of selected statistical parameters is shown in Table 2. All statistical parameters were obtained from the time AE signatures. If observed on the crack incubation stage, The mean value of standard deviation from AE2T and AE2C group are 0.03011 and 0.02667 respectively. The values were increased to 0.0566 for AEPT group and 0.0568 for AEPB group during microplastic and slip plane formation. During crack propagation, the mean of standard deviation of the AECP group increased. When the crack opening and closuse phenomena exist, standard deviation from AEOC group was dropped. The standard deviation from AECC group corresponds to compressed crack observed the lowest value. AE maximum amplitude and energy,

mean of standard deviation from the normal operating gas pipeline is higher than the fatigue mechanism. During crack propagation and crack opening and close, AECP and AEOC group shows high kurtosis. The trend of standard deviation mean value are similar to the trend from AE maximum amplitude and energy. Therefore, it can be concluded that standard deviation values are able to differentiate different stages of fatigue mechanism. In contrast, the trend of kurtosis of time domain, AE signatures from fatigue mechanism are not show an obvious different. Even that, it could separate between in-operation gas pipeline and crack stage, correspond to AECP and AEOC groups. It can be observed that the skewness value directly related with loading direction. During tension mode of cyclic stress, the skewness of AE2T, AEPT, AECP and AEOC groups given the positive values whereas for AE2C, AEPB and AECC groups given the negative value. It indicates that the normal operating condition load acting on tension due to the positive value of skewness of AEFM group. It is found that skewness can also detect the crack stage as well as kurtosis when fatigue mechanicsm with tensile mode.

Table 2. Range and mean value of standard deviation, kurtosis and skewness.

Signal Group	Standard Deviation	Mean of Standard Deviation	Kurtosis	Mean of Kurtosis	Skewness	Mean of Skewness
AE2T	0.0264 - 0.03425	0.0301	9.8 - 30.15	22.77	-0.623 – 0.664	0.0082
AE2C	0.0212 - 0.0351	0.0267	7.71 - 30.32	12.92	-0.45 – 0.538	-0.056
AEPT	0.0528 - 0.0602	0.0566	9.22 - 11.34	10	-0.236 – 0.374	0.065
AEPB	0.0315 - 0.1078	0.0568	6.53 - 48.92	21.75	-1.462 – 0.103	-0.286
AECP	0.098 - 0.1551	0.1237	38.35 - 49.35	45.75	0.82 – 1.467	1.132
AEOC	0.0392 - 0.077	0.048	23.8 - 63.37	44.41	-0.581 – 1.02	0.34
AECC	0.017 - 0.0282	0.022	9.12 - 29.44	17.55	-1.046 – 0.996	-0.105
AEFM	0.177 - 0.276	0.228	10.48 - 33.13	20.64	-0.713 – 2.446	0.774

CONCLUSIONS

Monitoring and assessment of the time domain AE signatures during fatigue mechanismand in-operation gas pipeline has been carried out. The distribution of AE counts during fatigue mechanism can be divided into three different stages including crack incubation stage, microplastic and slip plane formation stage and crack formation and propagation stage. The larger amplitude loading shorten the crack incubation stage. Crack initiations indicated by rapid increased of AE activities at positive peak stress. AE activities around zero stresses correspond as crack closure phenomena. AE maximum amplitude and energy from the normal operating pipeline show higher value than crack propagation. This phenomena is not suitable for condition monitoring purpose. Analysis of the kurtosis separate signatures from normal operating pipeline and crack propagation and crack closure. Skewness is a good parameter in separating signatures from different load directions. However, it is still not suitable to differentiate signatures from normal operating pipeline and fatigue mechanism. AE dominant frequencies found to separate signatures from fatigue mechanism and normal operating pipeline. Kurtosis is also promising to detect the micro phenomena during crack stage.

REFERENCES

Ai, Q., Liu, C.X., Chen, X.R. He P. and Wang, Y. 2010. Acoustic emission of fatigue crack in pressure pipe under cyclic pressure. Nuclear Engineering and Design. 240: 3616-3620.

Baranov, V., Kudryavtsev, E., Sarychev, G. and Shcavelin, V. 2007. Acoustic emission in friction. First ed. United Kingdom: Elsevier.

Berkovits, A. and Fang, D. 1995. Study of fatigue crack characteristic by acoustic emission. Engineering Fracture Mechanics, 51(3): 401-406.

Chan, K.S. 2009. Roles of microstructure in fatigue crack initiation. International Journal of Fatigue, 32(9): 1428–1447.

Chang, H., Han, E.H., Wang, J.Q. and Ke, W. 2009. Acoustic emission study of fatigue crack closure of physical short and long cracks for aluminum alloy LY12CZ, International Journal of Fatigue, 31: 403-407.

Elangovan, M., BabuDevasenapati, S., Sakhtivel, N.R. and Ramachandran, K.I. 2011. Evaluation of expert system for condition monitoring of a single point cutting tool using principle component analysis and decision tree algorithm. Expert System with Application, 38: 4450-4459.

Huang, M., Jiang, L., Liaw, P.K., Brooks, C.R., Seelay, R. and Klarstrom, D.L. 1998. Using acoustic emission in fatigue and fracture materials research. JOMe. 50(11):1.

Janssen, M., Zuidema, J. and Wanhill, R.J.H. 2004. Fracture mechanic. 2nd Edition. London: Spon Press.

Kalyanasundaram, P., Mudhophadyay, C.K., SubraRao, S.V. 2007. Practical acoustic emission. First ed. United Kingdom: Alpha Science International Ltd..

Lee, C.S., Rhyim, Y.M., Kwon, D. and Ono, K. 1995. Acoustic emission measurement of fatigue crack closure, ScriptaMetallurgicaet. Materialia. 32(5): 701-706.

Maslov, L.I. and Gradov, O.M.1986. Fracture energy analysis via acoustic emission. International Journal of Fatigue, 8(2): 67-71.

Muhlbauer, W.K. 2004. Pipeline Risk Management: Ideas, Techniques and Resources, Third ed. United States: Gulf Professional Publishing.

Nuawi, M.Z., Abdullah, S., Abdullah, S., Haris, S.M. and Arifin, A.K. 2009. MATLAB: A Comprehensive reference for engineers. First Edition, Malaysia: McGraw Hill.

Roberts, T.M. and Talebzadeh, M. 2003. Acoustic emission monitoring of fatigue crack propagation. Journal of Constructional Steel Research, 59: 695-712.

Zhong, Y. Shan, Y., Xiao, F. and Yang, K. 2005. Effect of toughness on low cycle fatigue behavior of pipeline steels. Material Letters, 59(14-15):1780-1784.